Experimental Determination of Damping Characteristics for a Single Flexible Link

Ashish Mohan[1*], S. P. Singh[2], S. K. Saha[3],

[1] Research Associate, Hi-Tech Robotic Systemz Limited, Gurgaon, India

[2] Associate Professor, Department of Mechanical Engineering, Indian Institute of Technology Delhi, New Delhi, India

[3] Professor, Department of Mechanical Engineering, Indian Institute of Technology Delhi, New Delhi, India. Presently with on-lien leave to IIT Madras, Chennai, India

[*] Corresponding author (email: ashishsept13@rediffmail.com)

Abstract

In this paper, a methodology and procedure for the experimental determination of the damping coefficients in the rigid-flexible robotic systems is presented. A brief overview of the work done by various researchers to theorically quantify the damping parameters is presented underlining the need to complement the theoretical estimation with the experimental data for accurate measurement of damping coefficients. The equations of motion of the rigid-flexible robotic systems incorporating damping are also outlined.

Keywords: Flexible, damping, logarithmic decay, method of evolving spectra

1 Introduction

Dynamics of a flexible link manipulator is highly non-linear, configuration dependent and computationally complex. Moreover, real robotic systems always involve external factors such as joint damping, structural damping in the flexible links, working environment of the robot, etc., which cannot be modeled without reasonable assumptions. As a result, the dynamic equations of the rigid-flexible robots, like the ones presented in [1-3], represent only idealized and approximate models of the actual systems. Attempts by various researchers [4-6] to theoretically estimate the damping factors of a system have been only partially successful. Consequently, experiments have generally been conducted by the different researchers to quantify the above physical parameters which cannot be easily modeled in the dynamic equations. The overall objectives of the experiments conducted are (i) to incorporate damping into the model, and (ii) to validate the theoretical model. Thus, Mingli et al. [7] have conducted experiments on a two flexible-link arm to identify the damping charecteristics in the motion and overall friction coming on the robot. Chapnik et al. [8] have experimentally investi-gated the projectile impact dynamics of an unactuated flexible beam. Feliu et al. [9] have conducted the experiments on a three degree of freedom robot to control its position using sensors and feedback loops. Mavroidis et al. [10] and Stieber et al. [11] have conducted experiments on the multi-link robot whose end effector is supported on a long and flexible link. Similarly, De Luca and Siciliano [12] have used the experimental results to study the regulation of the flexible arms under gravity. Similarly, Bragliato [13], Queiroz et al. [14] and Feliu et al. [15] have validated the dynamic models proposed by them using experimental verifications, and extended the results for feedback control. The results of the experiments are complemented with the theoretical models to estimate more accurate behavior of the robotic systems. Different experimental methodologies adopted by the above researchers vary mainly in its approaches, e.g., the type of sensors to measure vibrations, architecture of the robot, initial conditions, etc., and make trade-offs amongst the contradicting requirements. For example, while the frequency of rotational joint oscillations is moderate, the frequency of the vibrations of the flexible link is very high, hence it is difficult to measure both using a single sensor. Consequently, various researchers have adopted different combination of sensors, data acquisition systems, and actuators to study the tip performance characteristics. Also note that, a study conducted under open-loop control provides a better scenario for simulation validation since the use of feedback tends to mask some of the flexibility effects present in the system [16]. Moreover, the inclusion of damping in the dynamic model also improves the numerical stability characteristics of the simulation algorithm [1].

It is clear from the above that the study of damping, its estimation and incorporation into the real robotic systems is an area of research and has wide interest. Note that a robotic system has damping mainly because of two reasons: (1) due to friction at the joint assembly, namely joint damping; and (2) due to structural stiffness of its links, namely structural damping, which manifest itself physically in the form of decay in the amplitude of vibrations of the link. The experimental procedure presented in this paper for the determination of joint damping coefficients, is based on the logarithmic decay of the amplitude of the

oscillations of robotic links. The structural damping coefficients are estimated mainly using the modal analysis and the method of evolving spectra. First the effects of damping in different modes of vibrations are decoupled using the modal analysis. Then using the fast Fourier transform of the vibration response on the flexible in progressive time windows, the structural damping coefficients are determined. The advantage of the proposed method of determination of structural damping is that besides being accurate, it also provides information about the time-based amplitude of the vibration in each mode. The method is illustrated using a single flexible link clamped at one end. Comparison of the experimental results with the simulation results is also presented.

The paper is organized as follows: after a brief introduction and overview of the related work done by various researchers in Section 1, the dynamic equations of rigid-flexible robotic systems incorporating the damping are outlined in Section 2. Procedures proposed for estimation of damping coefficients, joint and structural, are presented in Section 3. The method of evolving spectra is also presented in Section 3 and the proposed method of estimation of structural damping coefficients is illustrated in Section 4 using a cantilever type flexible link, clamped at one end undergoing natural vibrations. As a simple representative of robotic systems with both joint and structural damping, example of a single flexible link with revolute joint and falling freely under gravity is presented in Section 5. Details of experimental set-up and comparison of experimental and simulation results are also presented followed by conclusions in Section 6.

2 Dynamic Equations of a Damped Robotic System

In a robotic system with rigid links the damping results mainly due to joint assembly, however damping in a flexible link is of two types: joint damping and structural damping. The decay in the amplitude of the oscillations of a link is due to friction at its joint, and is referred to as joint damping, whereas the decay in the amplitude of vibrations of a flexible link is due to its structural stiffness, and is called as structural damping. Both the types of damping characteristics are directly proportional to the first derivative (rate) of the associated generalized coordinates. For a rigid link, structural damping is absent as the generalized coordinates associated with the vibrations of the link do not exist. Moreover, only linear model of damping is considered here, for simplicity.

Dynamic equations of motion for a damped, n-link rigid-flexible serial robot are given as,

$$\mathbf{I}\ddot{\mathbf{q}} = \boldsymbol{\phi} + \mathbf{Z}\dot{\mathbf{q}} \qquad (1)$$

where $\dot{\mathbf{q}}$ is the $\bar{n}$ –dimensional vector of joint rates defined as

$$\dot{\mathbf{q}} \equiv \begin{bmatrix} \dot{\mathbf{q}}_1^T & \cdots & \dot{\mathbf{q}}_n^T \end{bmatrix}^T, \text{ and } \dot{\mathbf{q}}_i \equiv \begin{bmatrix} \dot{\theta}_i & \dot{\mathbf{d}}_i^T & \dot{\mathbf{c}}_i^T \end{bmatrix}^T$$

for $i=1, \ldots, n$, in which $\dot{\theta}_i$ is the rate of rotational or translational displacement of the ith joint, θ_i, depending on its type, i.e., revolute or prismatic, respectively. Vectors

$\dot{\mathbf{d}}_i$ and $\dot{\mathbf{c}}_i$ are the rates of generalized coordinates $\mathbf{d}_i$ and $\mathbf{c}_i$. Moreover $\mathbf{I}$ is the $\bar{n} \times \bar{n}$ Generalized Inertia Matrix (GIM), and $\boldsymbol{\phi}$ is the $\bar{n}$ –dimensional vector corresponding to the external generalized torques, convective and Coriolis terms, i.e., the quadratic terms of joint rates and derivatives of the flexible coordinates, and those associated with the potential, strain and dissipation energy terms. Furthermore, $\mathbf{q}$ is the vector of generalized coordinates associated with the joint angles or displacements, and those of the vibration amplitudes for the flexible links. Note that $\bar{n}$ is the degree of freedom (DOF) of the rigid-flexible robot given by, $\bar{n} \equiv n + \sum_{i=1}^{n_f}(3m_i + \overline{m}_i)$, where $n \equiv n_r + n_f$, is the total number of links– n_r and n_f being the number of rigid and flexible links, respectively. The scalars, m_i and $\overline{m}_i$ are the number of modes of vibration considered to model the link deflections in bending and torsion, respectively. Also, the number 3 in the formula for $\bar{n}$ corresponds to the X, Y and Z components of the spatial 3-dimensional deflection of the ith flexible link, and its corresponding generalized coordinates in bending are d_i^x, d_i^y and d_i^z. In this paper, for the purpose of ease of presentation the flexible links are considered planar, although the methodology presented is equally valid and can be easily extended to the general case of flexible beams undergoing vibrations in 3-dimensional space. Thus, the links are assumed to be vibrating in m_i number of modes about the joint axis, say Z-axis. Accordingly, for the systems at hand, $\bar{n}$ is given by $\bar{n} \equiv n + \sum_{i=1}^{n_f}(m_i + \overline{m}_i)$, and in eq. (1) the $\bar{n} \times \bar{n}$ damping coefficient matrix, $\mathbf{Z}$, is represented as

$$\mathbf{Z} = \begin{bmatrix} \mathbf{Z}_1 & \cdots & \mathbf{O} \\ \vdots & \ddots & \\ \mathbf{O} & & \mathbf{Z}_n \end{bmatrix} \qquad (2a)$$

where $\mathbf{Z}_i$, for $i=1, \ldots, n$, is the $(1+m_i+\overline{m}_i)$-dimensional matrix given by

$$\mathbf{Z}_i = \begin{bmatrix} \kappa_i & \mathbf{0} \\ \mathbf{0} & \boldsymbol{\zeta}_i \end{bmatrix} \qquad (2b)$$

in which the scalar κ_i represents the damping coefficient at the joint and the $(m_i + \overline{m}_i) \times (m_i + \overline{m}_i)$ dimensional diagonal matrix, $\boldsymbol{\zeta}_i$, corresponds to the structural damping of vibration of the link in m_i modes of bending and $\overline{m}_i$ modes of torsion. Note that, κ_i and $\boldsymbol{\zeta}_i$ are decoupled because of linear model of damping assumed here. Moreover, for rigid links, the damping coefficient matrix associated with link, i, namely $\mathbf{Z}_i$, reduce to a scalar κ_i. The joint damping coefficient κ_i and the elements of structural damping coefficients matrix $\boldsymbol{\zeta}_i$ are determined here from the experimental data.

3 Estimation of Damping Coefficients

In this Section, methodologies to determine the joint and structural damping coefficients are presented.

3.1 Joint damping

The joint damping coefficient, κ_i, for a robotic system can be given by

$$\kappa_i = \xi_i \bar{\kappa}_i \tag{3a}$$

where ξ_i is the damping ratio and $\bar{\kappa}_i$ is the critical damping factor associated with the ith joint. The damping ratio, ξ_i, is determined by measuring the rate of logarithmic decay of the oscillations of the link and is given by [17]

$$\xi_i = \{1/2\pi(k-1)\}\log_e(x_1/x_k) \tag{3b}$$

in which x_i and x_k are respectively the amplitudes in 1st and k^{th} cycles of oscillation of the link. The critical damping factor associated with the ith joint, $\bar{\kappa}_i$, is obtained as [17]

$$\bar{\kappa}_i = 4\pi\rho_i a_i \eta_f \tag{3c}$$

where ρ_i is the mass per unit length, a_i is the length–one of the four Denavit Hartenberg (DH)-parameters used to define a robots geometry– and η_f is the natural frequency of oscillation of the ith link.

3.2 Structural damping

The vibration amplitude of a flexible link is a combination of several modes. In order to determine the structural damping coefficients with respect to each individual modes of vibrations, it is required to separate out the decay in amplitudes of vibration due to each mode. This decoupling is essential because the structural damping coefficient of a beam is different in each of its mode. For a beam, vibrating in m_i modes of vibrations in bending and $\bar{m}_i$ modes of vibrations in torsion, the associated structural damping coefficients are given by $(m_i + \bar{m}_i)$ diagonal elements of the $(m_i + \bar{m}_i)\times(m_i + \bar{m}_i)$ diagonal matrix, ζ_i of eq. (2b). Similar to the joint damping, eq. (3a), the matrix for the structural damping coefficients is defined as:

$$\zeta_i = \tilde{\xi}_i \bar{\zeta}_i \tag{4a}$$

where $\tilde{\xi}_i$ is the $(m_i + \bar{m}_i)\times(m_i + \bar{m}_i)$ diagonal matrix of damping ratios associated with the m_i modes of vibrations in bending and $\bar{m}_i$ modes of vibrations in torsion of the ith link, and $\bar{\zeta}_i$ is the $(m_i + \bar{m}_i)\times(m_i + \bar{m}_i)$ matrix of critical damping factors associated with the respective modes. The matrices $\tilde{\xi}_i$ and $\bar{\zeta}_i$ are thus defined as,

$$\tilde{\xi}_i = \begin{bmatrix} \tilde{\xi}_{i1} & \cdots & & 0 \\ \vdots & \ddots & & \\ \vdots & & \tilde{\xi}_{ij} & \\ 0 & & & \tilde{\xi}_{iC} \end{bmatrix} \quad \bar{\zeta}_i = \begin{bmatrix} \bar{\zeta}_{i1} & \cdots & & 0 \\ \vdots & \ddots & & \\ \vdots & & \bar{\zeta}_{ij} & \\ 0 & & & \bar{\zeta}_{iC} \end{bmatrix} \tag{4b}$$

where $\tilde{\xi}_{ij}$, for j=1, …, m_i, is the damping ratio of the ith link in its jth mode, referred here as the modal damping ratio, and $\tilde{\xi}_{iC}$ is the $\bar{m}_i \times \bar{m}_i$ damping ratio matrix associated with the vibration of the ith link in torsion. In order to isolate the decay in the amplitude of vibration of link in each mode and to determine the corresponding damping ratios $\tilde{\xi}_{ij}$, the method of evolving spectra [18] is adopted here, whereas the critical damping factor, $\bar{\zeta}_{ij}$, for j=1, …, m_i, is obtained from the modal analysis of the link [17]. In this paper, for the comparison of experimental and simulation results, the torsional vibration is neglected due to the types of beams selected in the experimental set-up. Hence, the damping ratio matrix, $\tilde{\xi}_{iC}$, vanishes.

3.2.1 Structural damping ratios: Method of Evolving Spectra

In this section the method of determination of the $(m_i + \bar{m}_i)\times(m_i + \bar{m}_i)$ dimensional diagonal matrix of the structural damping ratios, $\tilde{\xi}_i$, associated with the m_i modes of vibrations in bending of the ith link is presented. The methodology, namely the method of evolving spectra, is based on the Fast Fourier Transform (FFT) of the response of the link in a series of selected time windows. First a time window is selected in the amplitude response of the link. Then the FFT of the response in this time window is performed. The natural frequencies of the link, known in advance from a real time analyzer, are identified as the sharp peaks in the FFT response. Thus, the corresponding amplitude of the link vibration in each mode is obtained. The time window is then shifted forward and FFT of the response in the shifted time window is performed again. The amplitude corresponding to each mode is then noted for this shifted position of time window. The process is repeated several times by shifting the time windows progressively. The amplitudes of the FFT curves corresponding to a particular mode in each time window are then plotted. It is found that the decay curve for the amplitudes corresponding to a mode is logarithmic in nature, which provides the structural damping ratio as,

$$\tilde{\xi}_{ij} = (1/2\pi\eta_j \Delta t_k)\log_e(x_{j1}/x_{jk}) \tag{5}$$

where η_j is the natural frequency of vibration of ith link in its jth mode, and x_{j1} and x_{jk} are the amplitudes of the vibrations in the 1st and k^{th} time windows of the response. Moreover, Δt_k is the shift in time for the kth time window with respect to the first time window. Alternatively, the amplitude decay of the peaks of the FFT curves for the corresponding frequencies are plotted against time on a semi-logarithmic scale. The slope of the curve divided by the corresponding natural frequency of the mode gives the structural damping ratio for the particular mode at hand. The method is now illustrated in Section 4 using example of a single flexible link clamped at one end and undergoing natural vibrations.

3.2.2 Critical damping factor: Modal analysis

The matrix of critical structural damping factors, $\bar{\zeta}_i$ of eq. (4b), is obtained here by the modal analysis of the link and is given by

$$\zeta_i = 2\sqrt{\widetilde{K}_{di}\widetilde{M}_{di}} \tag{6a}$$

where the $(m_i + \overline{m}_i) \times (m_i + \overline{m}_i)$ dimensional diagonal matrices, $\widetilde{K}_{di}$ and $\widetilde{M}_{di}$, are respectively the modal stiffness and modal mass matrices of the ith link. For a link vibrating in space in all three directions, namely, X, Y and Z, in m_i modes, $\widetilde{K}_{di}$ and $\widetilde{M}_{di}$ are the $(3m_i + \overline{m}_i) \times (3m_i + \overline{m}_i)$ matrices, which can be written using the modal analysis as

$$\widetilde{K}_{di} \equiv \int_0^{a_i} E_i I_i \begin{bmatrix} \overline{S}_i^x & & & \\ & \overline{S}_i^y & & \\ & & \overline{S}_i^z & \\ & & & O_{\overline{m}_i} \end{bmatrix}^{\mathrm{T}} \begin{bmatrix} \overline{S}_i^x & & & \\ & \overline{S}_i^y & & \\ & & \overline{S}_i^z & \\ & & & O_{\overline{m}_i} \end{bmatrix} d\overline{a}_{i+1} \tag{6b}$$

$$\widetilde{M}_{di} \equiv \int_0^{a_i} \rho_i \begin{bmatrix} S_i^x & & & \\ & S_i^y & & \\ & & S_i^z & \\ & & & O_{\overline{m}_i} \end{bmatrix} \begin{bmatrix} S_i^x & & & \\ & S_i^y & & \\ & & S_i^z & \\ & & & O_{\overline{m}_i} \end{bmatrix} d\overline{a}_{i+1} \tag{6c}$$

where $E_i I_i$ and ρ_i are respectively the flexure stiffness and mass per unit length of the ith link, and $O_{\overline{m}_i}$ is the $\overline{m}_i \times \overline{m}_i$ zero matrix due to the absence of torsional vibration. The $m_i \times m_i$ dimensional matrices, $\overline{S}_i^x$, $\overline{S}_i^y$ and $\overline{S}_i^z$; and S_i^x, S_i^y, and S_i^z, are the matrices associated with the shape functions for the vibrations about $\hat{X}_{i+1}$-, $\hat{Y}_{i+1}$- and $\hat{Z}_{i+1}$- axis: The axes are indicated in Fig. 1. Thus,

$$\overline{S}_i^x \equiv \begin{bmatrix} \dfrac{\partial s_{i,1}^x}{\partial \overline{a}_i} & & O \\ & \ddots & \\ O & & \dfrac{\partial s_{i,m_i}^x}{\partial \overline{a}_i} \end{bmatrix}; \quad S_i^x \equiv \begin{bmatrix} s_{i,1}^x & & O \\ & \ddots & \\ O & & s_{i,m_i}^x \end{bmatrix} \tag{6d}$$

where for, $j=1,...,m_i$, $s_{i,j}^x$ is the shape function of the ith link in its jth mode. The $m_i \times m_i$ dimensional matrices S_i^y, S_i^z, $\overline{S}_i^y$, and $\overline{S}_i^z$ are defined similarly for the shape functions associated with vibrations about $\hat{Y}_{i+1}$ and $\hat{Z}_{i+1}$-axes. As mentioned above, the links are considered to vibrate about the joint axis only, the vibrations about $\hat{X}_{i+1}$, $\hat{Y}_{i+1}$ − axes are neglected, i.e., the matrices, S_i^x, S_i^y, $\overline{S}_i^x$, and $\overline{S}_i^y$ vanish, and $\widetilde{K}_{di}$ and $\widetilde{M}_{di}$ become $(m_i + \overline{m}_i) \times (m_i + \overline{m}_i)$ dimensional matrices
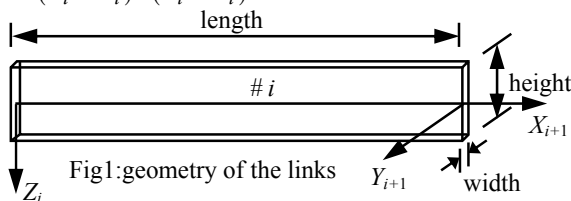

Fig1:geometry of the links

that are expressed as

$$\widetilde{K}_{di} \equiv \int_0^{a_i} E_i I_i \begin{bmatrix} \overline{S}_i^z & \\ & O_{\overline{m}_i} \end{bmatrix}^{\mathrm{T}} \begin{bmatrix} \overline{S}_i^z & \\ & O_{\overline{m}_i} \end{bmatrix} d\overline{a}_{i+1} \tag{6e}$$

$$\widetilde{M}_{di} \equiv \int_0^{a_i} \rho_i \begin{bmatrix} S_i^z & \\ & O_{\overline{m}_i} \end{bmatrix}^{T} \begin{bmatrix} S_i^z & \\ & O_{\overline{m}_i} \end{bmatrix} d\overline{a}_{i+1} \tag{6f}$$

where $m_i \times m_i$ dimensional matrices $\overline{S}_i^z$ and S_i^z, are defined similar to eq. (6d).

4 An Illustration:

First the method of determining joint damping coefficients is presented, followed by the structural damping coefficients of damping coefficients

4.1 Joint damping

The method of determination of the joint damping coefficient, κ_i, as presented in Section 3.1, is now illustrated using an example of a single rigid link falling freely under gravity. The only scalar equation of motion represented in the form of eq. (1) is given by $\rho a^3 \ddot{\theta}/3 = \tau + \kappa \dot{\theta}$ where ρ, a, θ, and τ are respectively the mass per unit length, link length, joint angle, and the external torque due to gravity, whereas κ is the associated joint damping coefficient of the system, that will be determined from the experimental data and using eqs. (3a-c). The scheme of the experiment conducted is shown in Fig. 2 using a 0.33m long, carbon steel beam with cross-section 0.018×0.004m2 and mass 0.180Kg, hinged by a revolute joint. The angular displacement of the link is measured using the 10 KΩ, ±0.25% linearity, wire-wound pot wire-pot potentiometer, mounted at the joint. The link is allowed to fall freely under gravity from an initial position of 7° from the vertical. The corresponding angular displacement of the link, as measured by the potentiometer, is shown in Fig. 3. The ratio of the successive amplitudes of oscillations is obtained from it and used in eqs. (3b) to obtain the damping ratio, $\xi_1 = 0.0142$, whereas the critical damping factor associated with the joint, namely, $\overline{\kappa}_1$, is obtained from eq. (3c) using the physical parameters of the link and its
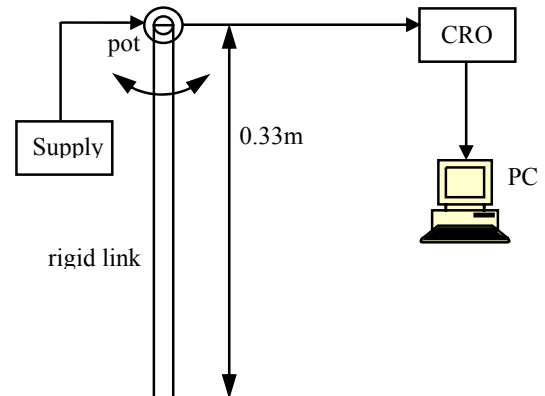

Figure 2 Experimental set-up for the single rigid link

natural frequency, η_f, as obtained from the experimental results. The value of $\bar{\kappa}_1 = 2.1716$ Kg/s . The joint damping coefficient, κ_1, is then obtained from eq. (3a) as 0.0308 Kg/s for the single rigid link under study. The joint damping coefficient, κ_1, is next incorporated into eq. (1) and the simulation for the same initial conditions is repeated. The resulting angular variation is plotted in Fig. 3 and compared with those obtained from the experiments. It is seen that the experimental and simulation results match closely, thus, verifying the modeling technique of the joint damping in the dynamic model. The frequency of oscillation is also obtained from the Fourier transform of the experimental response for the joint angles. This is obtained as 0.96Hz, while the frequency of oscillation of the link, as obtained from the simulation results is 1.0Hz, which is a good match.
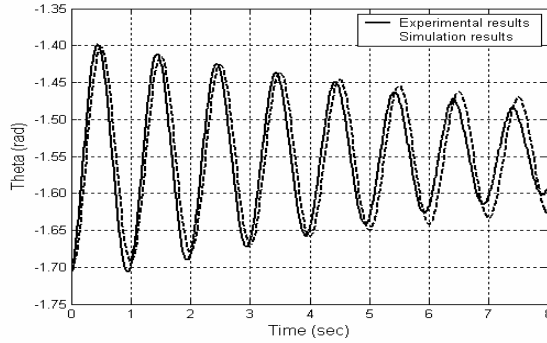
Figure 3: Simulation results for single rigid link

4.2 Structural damping

The method of determining structural damping coefficients, as presented above, is now illustrated using an example of a single flexible link. In order to illustrate the methodology for estimation of the damping due to structural stiffness of the links, vibrations of a cantilever type flexible beam, clamped at one end, Fig. 4 is considered under natural conditions. Since such a beam does not oscillate, i.e., does not have any joint motion, the joint damping is absent. Moreover, the beam is kept in such a way that it vibrates in vertical plane only. For the

Table 1: Experiment with a single flexible link
(a) Physical parameters of the link

Material	Length	Cross-section	Mass	Flexure stiffness
Spring steel	0.33m	$0.024\times0.001m^2$	0.060Kg	0.4 Nm^2

(b) Specifications of the equipments

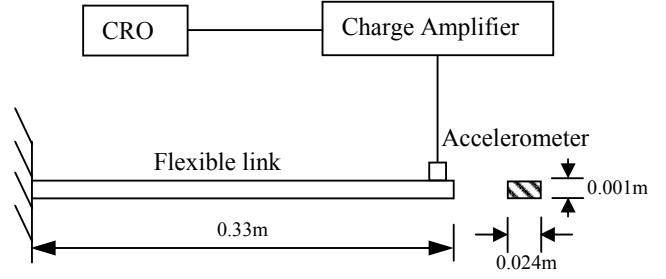| Equipment	Specifications
Accelerometer	$0.024\times0.001m^2$
Charge amplifier	Bruel and Kjaer, 2635; Lower frequency cut-off: 2Hz; Higher frequency cut-off: 30Hz; Calibration factor: 100mV/mm; Charge sensitivity: 1.003pC/ms^{-2}; Voltage sensitivity: 0.88mV/ms^{-2}
Data acquisition system	Agilent, 54621oscilloscope; 60MHz, 200MSa/s

Figure 4: A beam type link clamped at one end.

purpose of modeling, only first two modes are considered. Correspondingly, the determination of the structural damping coefficient in first two modes is shown here. The physical parameters of the link and the set-up are presented in Table 1. The physical dimensions and the mass properties of the link are so selected that the flexibility characteristics of the link are prominent. An accelerometer is mounted at the end of the beam, as indicated in Fig. 4 to record the amplitude response. The output of the accelerometer is amplified using a charge amplifier and the readings are taken on an oscilloscope.

For a single flexible link vibrating in its first two modes, equations of motion, eq. (1), are expressed as,

$$\rho\begin{bmatrix} \dfrac{a^3}{3}+k_{11}d_1^2+k_{12}d_2^2 & k_{21} & k_{22} \\ & k_{11} & \\ sym & & k_{12} \end{bmatrix}\begin{bmatrix} \ddot{\theta} \\ \ddot{d}_1 \\ \ddot{d}_2 \end{bmatrix}+\rho\begin{bmatrix} 2\dot{\theta}\left(k_{11}\dot{d}_1^2+k_{12}\dot{d}_2^2\right) \\ -k_{11}d_1\dot{\theta}^2 \\ -k_{12}d_2\dot{\theta}^2 \end{bmatrix}$$
(7a)

$$=\begin{bmatrix} \tau_\theta \\ \tau_{d_1}+\tau_{d_1}^s \\ \tau_{d_2}+\tau_{d_2}^s \end{bmatrix}+\begin{bmatrix} \kappa & 0 & 0 \\ & \zeta_1 & 0 \\ sym & & \zeta_2 \end{bmatrix}\begin{bmatrix} \dot{\theta} \\ \dot{d}_1 \\ \dot{d}_2 \end{bmatrix}$$

where ρ is the mass per unit length, a is the link length, θ is the joint angle, d_1 and d_2 are the generalized coordinates of the link vibrating in 1st and 2nd modes, respectively. Moreover, the terms, τ_θ, τ_{d_1} and τ_{d_2} are respectively the corresponding generalized forces corresponding to the generalized coordinates, θ, d_1 and d_2 . The terms, $\tau_{d_1}^s$ and $\tau_{d_2}^s$ are the terms due to strain energy. The expressions for $\tau_{d_1}^s$ and $\tau_{d_2}^s$ are given in [18, 19] , whereas k_{1j} and k_{2j}, for j=1, 2, are the constants associated with the shape functions, i.e.,

$$k_{1j} \equiv \int_0^a s_j^2 d\bar{a} \text{ and } k_{2j} \equiv \int_0^a s_j d\bar{a}$$
(7b)

in which s_j is the shape function of the link in j^{th} mode. Since there is only one link, i=1, which is omitted from the ensuing expressions to reduce clumsiness. Furthermore, κ is the joint damping coefficient, and ζ_j, for j=1, 2, is the associated structural damping coefficient of the link which

will be determined here from the experimental data. The scheme of the experiment is shown in Fig. 4. Corresponding to the two modes of vibrations, the structural damping coefficients are given by, $\zeta_j = \tilde{\xi}_j \bar{\zeta}_j$, for j=1,2, in which $\tilde{\xi}_j$ and $\bar{\zeta}_j$ are respectively the structural damping ratio and critical damping factor associated with vibration in the jth mode. To determine the structural damping coefficients of the link, tip of the link is deflected by a known displacement (0.015m) and released to vibrate in its natural condition. The amplitude decay curve of the link, as obtained from the accelerometer, is shown in Fig. 5(a). The structural damping coefficient, ζ_j, is then estimated by first determining the structural damping ratio $\tilde{\xi}_j$ using the method of evolving spectra explained in Sub-subsection 3.2.1. A time window of 0.05 sec is selected. Two such positions of the time window, namely, the 1st and 4th, are shown in Fig. 5(a). In order to eliminate the manual errors during initialization of experiments the data for damping is estimated from the response of the beam after 0.05s. FFT of the responses in different time windows are plotted to get Fig. 5(b). Figure 5(b) is called as the waterfall plot. For clarity of representation, FFT responses in only four locations of time window are shown. The peaks in the FFT curves are located corresponding to the natural frequencies of the link, the amplitudes of the successive peaks on a particular natural frequency are now noted. Since the determination of structural damping coefficients is performed for the first and second modes, amplitudes of the successive peaks, namely, x_1 and x_2 for the 1st mode, as shown in Fig. 5(b), are noted. Then, using eq. (5) the structural damping ratio $\tilde{\xi}_1$ is calculated. Note that, the first subscript i is omitted as there is only one link. Similarly, the ratio for the 2nd mode, $\tilde{\xi}_2$, is obtained. Alternatively, the amplitude decay of the peaks of the FFT curves for the 1st and 2nd natural frequencies are plotted against time on a semi-logarithmic scale, as shown in Fig. 5(c). The slope of the curve divided by the corresponding natural frequency of the mode gives the structural damping ratio for the particular mode at hand. For the link under study, the latter methodology, i.e., Fig. 5(c), is used, which results in $\tilde{\xi}_1 = 0.1980$ and $\tilde{\xi}_2 = 0.0428$. Next, the critical damping ratios, $\bar{\zeta}_j$, for j=1, 2, are calculated using the link length a, the shape functions, and eq. (6a). The values are $\bar{\zeta}_1 = 6.9 \times 10^{-2}$ Kg/s and $\bar{\zeta}_2 = 6.5 \times 10^{-3}$ Kg/s. Finally, the structural damping coefficient, ζ_j, is obtained for j=1, 2,

using $\quad \zeta_j = \tilde{\xi}_j \bar{\zeta}_j \quad$ as $\quad \zeta_1 = 1.37 \times 10^{-2} \quad$ Kg/s

and $\zeta_2 = 2.8 \times 10^{-3}$ Kg/s. They are then incorporated into the eq. (7a). Simulation is then performed using eq. (7a) with the following initial conditions: Since the tip of the link is initially deflected by a known amount, $\boldsymbol{u}$, i.e,
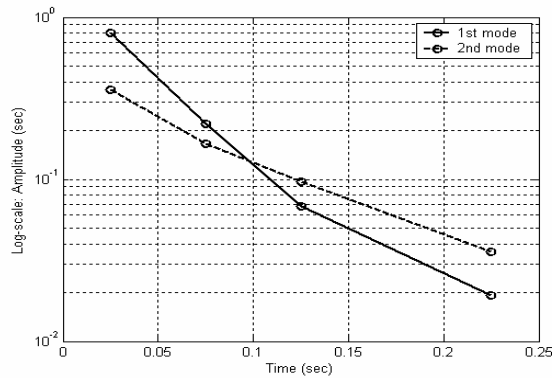
$$\boldsymbol{u} \equiv \begin{bmatrix} \bar{s}_1^z & 0 \\ 0 & \bar{s}_2^z \end{bmatrix} \begin{bmatrix} d_1 \\ d_2 \end{bmatrix} \tag{8}$$
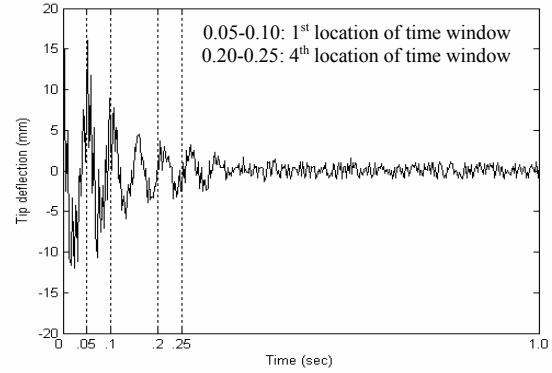
(a) Amplitude response of the tip
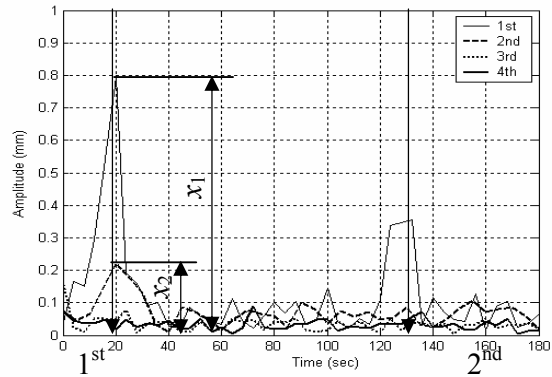
(b) FFT of the amplitude responses

(c) Decay of amplitude of vibrations

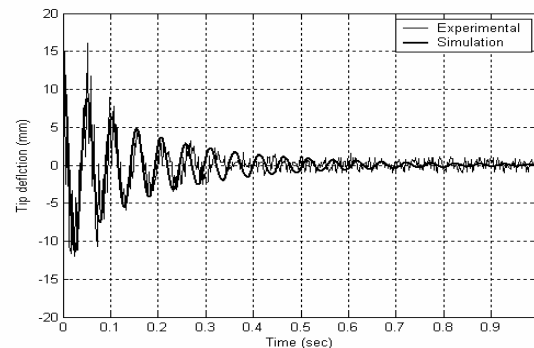Figure 5: Determination of structural damping ratio

Figure 6: Comparison of simulation and experimental results

where, for j=1, 2; $\bar{s}_j^z$ is the shape function associated with the bending of the link in jth mode and evaluated at a, i.e., the tip of the link, which is known. Assuming d_2=0, d_1 is evaluated. Now, in order to use eq. (7a) for the simulation, θ is always zero since one end of the link is clamped. Accordingly, $\dot{\theta} = \ddot{\theta} = 0$. Also, initially, $\dot{d}_1 = \dot{d}_2 = 0$. Simulation results for the tip-deflection of the link thus obtained are then compared with those obtained experimentally, as in Fig. 6. It is clear from the plots that the experimental and simulation results match closely, thus verifying the values for the structural damping coefficients as correct.

5 Simulation

In this section, a single flexible-link hinged on a revolute joint and falling freely under gravity is considered as a simple representative of a robotic system having both joint and structural damping. The simulation results, obtained using eq. (1), are presented and compared with the experimental results. The flexible link used as moving arm is the same as used in Subsection 4.2. The scheme of the experiment, to obtain the data corresponding to damping coefficients, is shown in Figs. 7. The physical parameters of the link and the experimental set-up are shown in Table 1(a). The joint displacement of the link is measured using a 10 KΩ, ±0.25% linearity, wire-wound potentiometer placed at the joint. The deflection at the tip of the link is measured using a full strain-gauge Wheatstone bridge mounted at the root of the link. Two 350Ω, 100% gain, strain gauges are mounted on each side of the link so that the proper conditioning of the readings is obtained giving the deflection direction correctly. The strain-gauge signals are amplified using an ADAM-3016, DIN rail-mounted, amplifier and the output is taken on the PICO CRO with Pentium IV Intel processor computer. The strain gauge readings are calibrated by giving beam a series of known deflections and measuring the corresponding strain gauge readings. It is seen that the bridge exhibits linear characteristics in the range of deflection [19]. To perform the experiment, the link is allowed to fall freely under gravity from the horizontal position, as per Fig. 7, with no initial deflection and no external torque applied on it. The angular displacement of the joint was measured by the potentiometer, and the tip deflection of the link using the
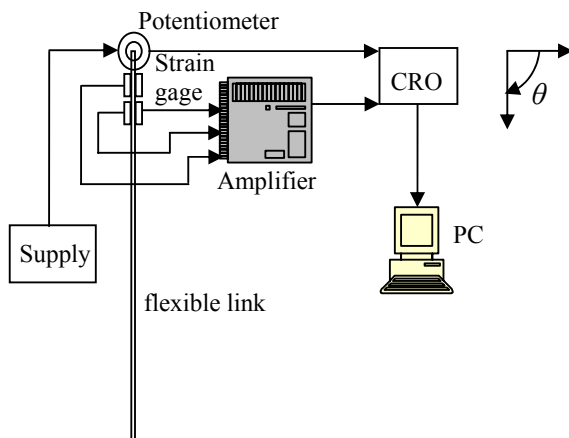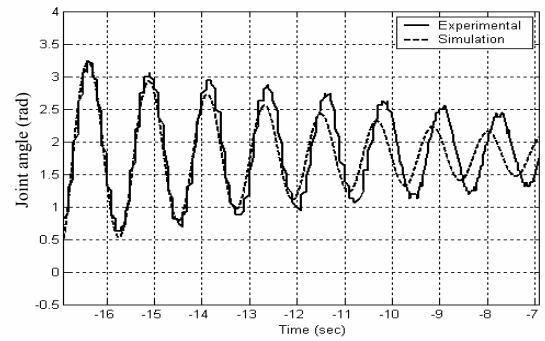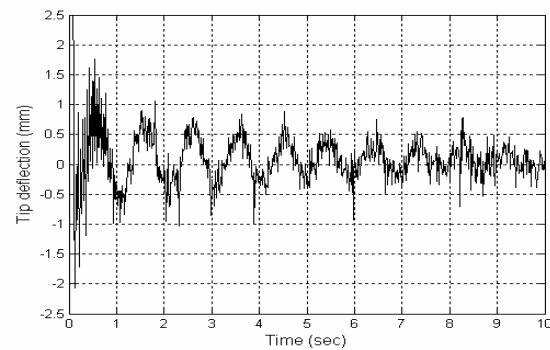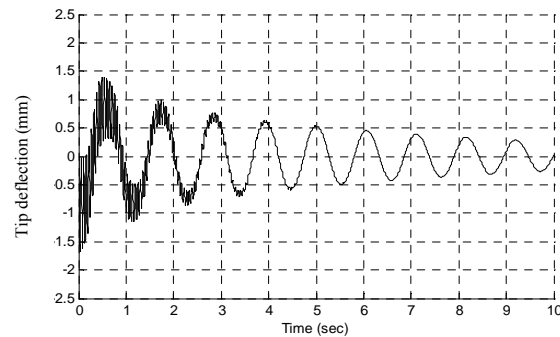

Figure 7: Experimental set-up for single flexible-link arm

(a) Joint angle

(b) Tip deflection : Experimental results

(c) Tip deflection : Simulation results
Figure 8: Free fall results of a single flexible link

strain-gauges. The results are shown in Fig. 8(a-b). To obtain the simulation results, joint damping coefficient, and structural damping are first calculated respectively as $\kappa = 0.0106$ Kg/s and $\zeta_1 = 1.37 \times 10^{-2}$ Kg/s, $\zeta_2 = 2.8 \times 10^{-3}$ Kg/s using the scheme presented in Section 3. The damping factors were then incorporated into eq. (7a) and the free-fall simulation results were obtained. Initial conditions for simulation are taken as, $\theta = d_1 = d_2 = 0; \dot{\theta} = \dot{d}_1 = \dot{d}_2 = 0$. Figures 8 (a-c) show the comparison of the experimental and simulation results for the joint angle and tip deflection of the link, respectively. The fast fourier transformation, i.e., FFT, of the experimental results, Figs. 8(a-b) show an oscillation frequency of 1.1Hz and the tip vibration frequency of 20.5Hz., respectively. From the simulation results, the joint oscillation and tip vibration frequencies are 1.1Hz is 21Hz, respectively. Also, the amplitudes of joint oscilla-

tions and tip vibrations also match closely, particularly during the first three-four cycles. The mismatch in the peak height values is attributed to the fact that the real beam vibrates in all possible modes of vibration, whereas the simulation considered only for first two modes of vibration. The worsening of results in the latter part is mainly due to linear decay considerations of the damping factors given by eqs. (3-4).

6 Conclusions

A methodology for the accurate estimation of the damping characteristics of rigid-flexible robotic systems, using the data obtained from a series of experiments, is presented here. Procedures for the determination of both joint and structural dampings are presented. The joint damping is estimated using the logarithmic decay of joint rotation. For measuring the structural damping, modal analysis is used to estimate the critical structural damping coefficient, and the method of evolving spectra to find the structural damping ratio. Since, for a flexible beam, the structural damping ratio corresponding to its various modes of vibrations are coupled with each other particular emphasis is laid on the proposed method of evolving spectra for the estimation of structural damping ratios. The method is also illustrated using a flexible beam, clamped at one of its ends, undergoing natural vibrations. It is shown that the experimental results match closely with simulation results. Typical advantages of the proposed method are as follows: 1) The method involves simple experiments which do not need any sophisticated equipments. Infact even with the simple equipments like accelerometer, strain-gauges, potentiometers, etc. it is possible to obtain the necessary data with fair accuracy. 2) The variation in the time varying amplitudes of the vibrations are obtained which is useful for building up the control algorithm for reduced vibration.

Acknowledgment

References

[1] Cyril, X., 1988, Dynamics of flexible link manipulators, Ph.D. dissertation, McGill University, Canada.

[2] De Luca, A., and Siciliano B., 1991, "Closed-form dynamic model of planar multilink lightweight robots," IEEE Trans. on Systems, Man and Cybernetics, vol. 21, no. 4, pp. 826-838.

[3] Mohan, A., and Saha, S. K., 2007, "A computationally efficient and numerically stable simulation algorithm for serial robots with flexible links," Proc. of Int. ECCOMAS Thematic Conference on multibody dynamics, Milano, Italy, 25-28 June.

[4] Lankarani, H. M., and Nikravesh, P. E., 1990, "A contact force model with hysteresis damping for impact analysis of multibody systems," ASME Journal of Mechanical Design, vol. 112, pp. 369-376.

[5] Ambrosio, J. A.C., and Rayn, P., 1997, "Elastodynamics of multibody systems using generalized inertial coordinates and structural damping," Journal of Mechanical Structural Mechanics, vol. 25, no. 2, pp. 201-219.

[6] Austin, E. M., and Inman, D. J., 2000, "Errors in damping predictions due to kinematic assumptions for sandwich beams," Proc. of Int. Conf. on Structural Dynamics–recent advances, pp. 515-526.

[7] Mingli, B., Zhou, D. H., and Schwarz H., 1999, "Identification of generalized friction for experimental planar two-link flexible manipulator using strong tracking filter," IEEE Trans. of Robotics and Automation, vol. 15, no.2, pp. 362-369.

[8] Chapnik, B. V., Heppler, G. R., and Aplevich, J. D., 1991, "Modeling impact on a one link-flexible robotic arm," IEEE Trans. on Robotics and Automation, vol. 7, no. 4, pp. 479-488.9 Feliu et al.

[9] Feliu, V., Garcia, A., and Somolinos, J. A., 2000, "Gauge-based tip position control of a new three degree of freedom flexible robot," Int. Journal of Robotics Research, vol. 20, no. 8, pp. 660-675.

[10] Mavroidis, C., Dubowsky, S., and Raju, V., 1995, "End-pont control of long reach manipulator systems," Proc. of IX World congress on Theory of Machines and Mechanisms, Milan, Sept 1-3.

[11] Stieber, M. E., McKay, M., Vukovich, G., and Petriu, E., 1999, "Vision based sensing and control for robotics appliactions," IEEE Trans. on Inst. and Measurement, vol. 48, no. 4, pp. 807-812.

[12] De Luca, A., and Siciliano B., 1993, "Regulation of flexible arms under gravity," IEEE Trans. on Robotics and Automation, vol. 9, no. 4, pp. 463-467.

[13] Bragliato, B., Rey, D., Pastore, J., and Barnier, J., 1998, "Experimental Comparision of Nonlinear Controllers for Flexible Joint Manipulators," Int. Journal of Robotics Research, vol. 17, no.3, pp 260-281.

[14] Queiroz, M. S., Donepudi, S., Burg, T., and Dawson, D. M., 1999, "Adaptive nonlinear boundary control of a flexible link robot arm," IEEE Trans. on Robotics and Automation, vol. 15, no. 4, pp. 779-787.

[15] Feliu J., Feliu V., and Cerrada C., 1999, "Load adaptive control of single-link flexible arms based on a new modeling technique," IEEE Trans. on Robotics and Automation, vol. 15, no. 5, pp. 793-814.

[16] Stanway, J., Sharf, I., and Damaren, C., 1996, "Validation of a dynamics simulation for a structurally flexible manipulator," Proc. of IEEE Conf. on Robotics and Automation, Minnestoa, pp. 1959-1964.

[17] Thompson, W. T., 1988, Theory of Vibration with Applications, Prentice Hall, London.

[18] McIntyre, M. E., and Woodhouse, J., 1988, " On measuring the elastic and damping constant of orthotropic sheet materials", ACTA Metal. vol. 36, no. 6, pp. 1137-1416.

[19] Mohan, A., 2006, Dynamic Analysis of flexible robotic systems, Ph.D. dissertation, Indian Institute of Technology Delhi, New Delhi, India.